**NURETH14-503** 

# THE US NRC ADVANCED GAS REACTOR EVALUATOR (AGREE) T.J. Drzewiecki<sup>1</sup>, V.Seker<sup>1</sup>, J. M. Kelly<sup>2</sup>, and T.J. Downar<sup>1</sup>

Department of Nuclear Engineering and Radiological Sciences
 University of Michigan, Ann Arbor, MI USA
 US Nuclear Regulatory Commission, Washington, D.C. USA
 tjdrzew@umich.edu, vseker@umich.edu, downar@umich.edu

#### Abstract

A Prismatic Module Reactor (PMR) core fluids model has been developed in support of the US NRC Next Generation Nuclear Plant (NGNP) evaluation model. The PMR core fluids modeling relies on a subchannel approach in which the primary coolant flowpath through the core region and vertical in-core and ex-core gaps can be modeled as individual subchannels. These subchannels are connected together to represent a three dimensional reactor. An initial validation calculation has been performed using data available in literature for bypass flow. The predicted bypass flow was within 2.6% of the value reported in the literature. Further verification and validation is awaiting the completion of the coupling of the fluids model with a triangular solid heat conduction model.

## 1. Introduction

The Advanced Gas REactor Evaluator (AGREE) was originally developed as a multiphysics simulation code to perform design and safety analysis of next generation Pebble Bed High Temperature Gas Cooled Reactors [1]. It utilizes a suite of code modules to solve the coupled thermal-fluids and neutronics field equations. The thermal-fluids module is based on the three dimensional solution of the mass, momentum, and energy equations in cylindrical coordinates within the framework of the porous media method. The neutronics module is a part of the PARCS code and provides a fine mesh finite difference solution of the neutron diffusion equation in three dimensional cylindrical coordinates [2]. Additional capabilities are being implemented into the original AGREE code in order to capture the necessary physics pertinent to PMRs. These capabilities are implemented through separate code modules pertaining to fluid flow and heat transfer. This paper focuses on the development and testing of the fluids module.

## 1.1 Approaches to PMR fluids modeling

After reviewing the necessary physics required for PMR core fluids modeling, a set of code requirements has been established for the fluid flow module. The key requirements are: calculation of core bypass flow, capturing the momentum flux term in the momentum equation, and the ability to handle flow reversals.

A Phenomena Identification and Ranking Table (PIRT) process has been completed for the NGNP [3]. The accident and thermal fluids PIRT panel has identified core coolant bypass flow as having an importance rank of high with a corresponding knowledge level of low. In the case of the PMR with the inter-block gaps, radial and axial manufacturing and refueling tolerances for the graphite blocks, irradiation swelling and cracking and the distribution of the thermal expansion, past experience and expertise indicates that the core bypass flow could be a significant proportion of the total core flow [4]. The bypass flow paths are located in the in-core and ex-core vertical columns between the stacks of

hexagonal graphite blocks and through control rod holes within the graphite blocks. Additionally, the coolant can pass between the primary coolant flow path and the bypass flow path through horizontal gaps formed between the stacked graphite blocks. Therefore, the core fluid flow is essentially three-dimensional.

Several approaches to modeling fluid flow though the core of a PMR have been utilized that range from flow networks to full 3D CFD simulation. Flow network codes such as FLOPSY [5] and GAS-NET [6], have been used by General Atomics and others to determine the flow distribution in the PMR core. These flow network codes are zero-dimensional in the sense that the convective terms are neglected and the solution represents a balance between pressure and friction forces. Neglecting the convective terms makes the solution computationally inexpensive, but these terms can be significant, especially during a transient (e.g. pressure wave propagation, flow-reversal, etc.). Another approach is to use existing 1D system codes such as RELAP, TRACE, etc. (i.e. RELAP5 has been utilized to study leakage flows through the PMR core [7]). 1D system codes have the benefit of a very flexible input structure and a history of successful use for the analysis of light water reactors. Implementation of 1D system codes for PMR analysis may require substantial modification to implement the appropriate bypass flow loss coefficients, and concern remains in regards to 3D flow modeling. Finally, literature is available that demonstrates 3D CFD modeling of the PMR [8], [9]. CFD provides high fidelity solutions and has been coupled with neutron transport codes [9]. The primary drawback to CFD analysis is the large computational expense associated with the relatively finely meshed computational domain. This large computational expense is amplified by the length of the transients that need to be performed for the PMR (i.e. peak kernel temperature for the DLOFC occurs days into the event). As a compromise between the 1D system codes and CFD, a subchannel approach has been selected as the basis to model PMR fluids in AGREE.

# 1.2 The subchannel approach

The subchannel approach divides the entire core into several subchannels, where each subchannel is representative of the flow in that specified region of the core. Each subchannel consists of several smaller volumes stacked axially upon each other. These subchannels can be connected to other subchannels in juxtaposition by specifying gaps. Gaps consist of several junctions that provide a flowpath between adjacent subchannels.

Calculating the axial momentum flux terms allows the code to capture the pressure and velocity changes that occur when flow acceleration is significant. This local acceleration can occur by area changes in the flowpath as well as expansion of the coolant due to heat transfer. Inclusion of the momentum flux terms results in non-linear partial differential equations which will be handled in the mathematical model.

The normal flow path of the coolant through the core is from the top of the core to the bottom of the core. In the Loss of Forced Circulation (LOFC) accident scenario natural circulation is anticipated to occur during the transient, where the coolant flows from the bottom of the core to the top of the core. Hence, during the LOFC event the coolant flow through the core will initially be relatively large in the normal direction, slow down to stagnation and then change direction. In order for the code to capture this change in flow direction, a hybrid differencing scheme will be used in the axial dimension. The hybrid differencing scheme is a combination of upwind differencing with zero diffusion and central differencing [10].

#### 2. The mathematical model

# 2.1 Application of the subchannel approach

In the subchannel approach, a three-dimensional core is represented by a series of cross-connected one-dimensional subchannels. As a visualization aid, a cluster of six graphite-elements is shown in Fig. 1 and Fig. 2, where each graphite-element is broken up into six individual subchannels and each bypass flowpath is represented as an individual subchannel.

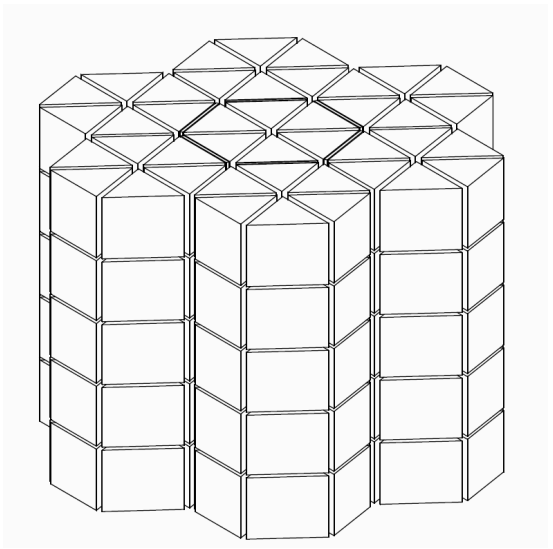


Fig. 1: Computational domain used in subchannel approach.

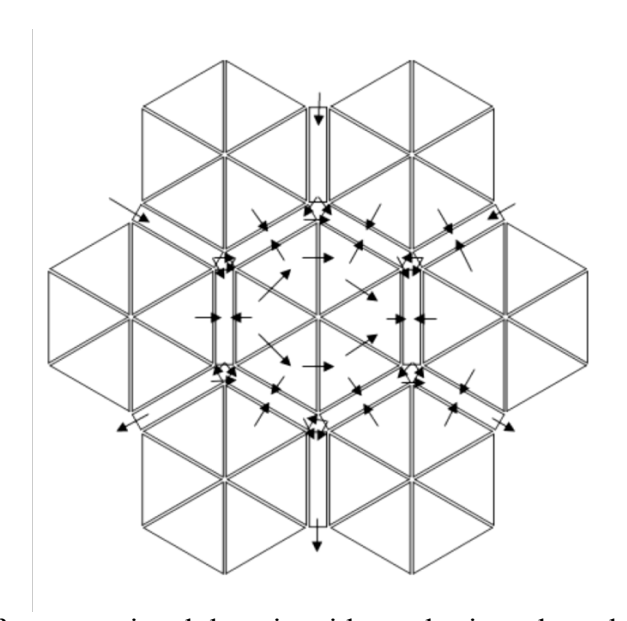


Fig. 2: Top view of computational domain with emphasis on lateral-flow junctions (gaps).

The velocity field is broken up into axial and lateral components. The axial component corresponds to the fluid flowing vertically through the core and utilizes a general momentum transport equation. The lateral component of momentum is aligned normal to the axial component, and an assumption is imposed that the lateral component of fluid flow is only significant near the lateral faces. Hence, the lateral flux terms are assumed to be negligible. The assumption imposed on the lateral momentum equation has its origins in the subchannel codes used successfully for Light Water Reactor (LWR) core thermal-hydraulic analysis, namely the COBRA [11] and VIPRE codes [12]. This assumption greatly simplifies the governing equations by reducing a fully-three-dimensional system to a network of 1-D subchannels and has been applied successfully for LWR analysis where the axial component of the flow is significantly larger than the lateral component of the flow.

#### 2.2 Treatment at block interfaces

The portrayal of lateral flow junctions shown in Fig. 2 demonstrates the radial locations of the junctions, but the axial locations of the junctions depend on what is being connected. The lateral junctions that connect bypass channels to adjacent bypass channels are placed at the lateral faces of the control volumes since these gaps are open along the entire length of the graphite block, and therefore do not impose any additional modelling concerns. Crossflow to or from the main coolant occurs at block faces, and therefore occurs at an axial face of a control volume and requires special treatment. Instead of placing a lateral junction at the top or bottom control volume within a graphite block, zero-volume nodes are placed between axially aligned components as shown in Fig. 3 and Fig. 4.

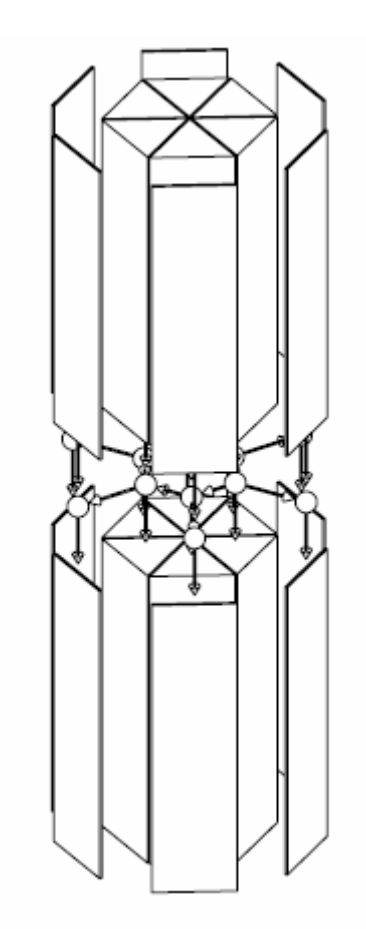


Fig. 3: Illustration of axial components connected through zero-volume nodes.

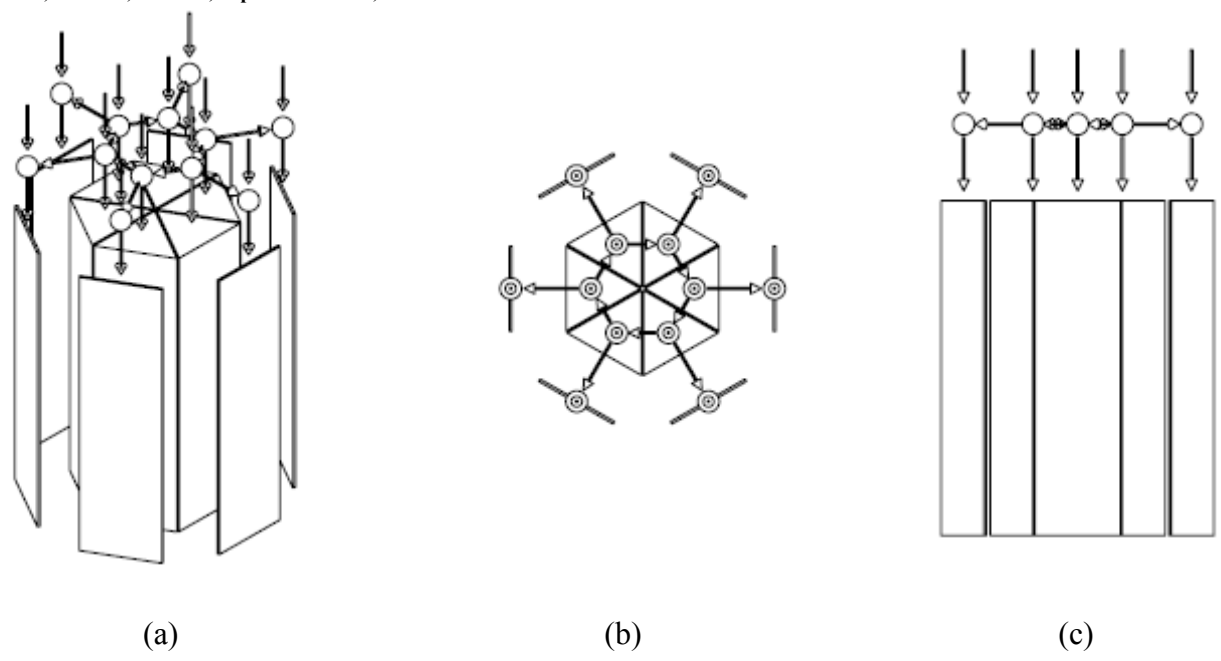


Fig. 4: Lateral junctions connecting zero volume nodes allowing for crossflow between coolant channels and between a coolant channel and bypass flow channel: (a) isometric view, (b) top view, (c) front view.

# 2.3 Transport equations

The control volume used in the derivation of the axial momentum, energy, and continuity equations is shown in Fig. 5. The shape of the control volume is arbitrary in the sense that there is no specified limit to the number of lateral-flow junctions that can be connected to a volume. The resulting transport equations are given below.

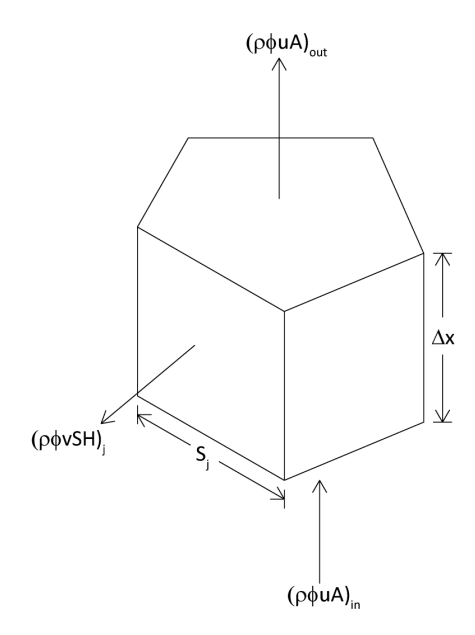


Fig. 5: Control volume used in derivation of axial momentum, energy, and continuity equations.

Continuity

$$\frac{A\Delta x}{\Delta t}\rho + (\rho uA)_{out} - (\rho uA)_{in} = -\sum_{j} (\rho vSH)_{j} + \frac{A\Delta x}{\Delta t}\rho^{0}$$
(1)

Conservation of Energy

$$\frac{A\Delta x}{\Delta t}(\rho h) + (\rho h u A)_{out} - (\rho h u A)_{in} = q''_{in} \xi_H \Delta x + \left(kA \frac{\partial T}{\partial x}\right)_{out} - \left(kA \frac{\partial T}{\partial x}\right)_{in} - \sum_j (\rho h v S H)_j + \frac{A\Delta x}{\Delta t}(\rho h)^0$$
(2)

Conservation of Axial Momentum

$$\frac{A\Delta x}{\Delta t}(\rho u) + \left(\rho u^2 A\right)_{ut} - \left(\rho u^2 A\right)_n = \left(p_{in} - p_{out}\right)A + \left(K + \frac{f l}{D_H}\right)\left(\rho \frac{|u|u}{2}A\right) - \sum_j \left(\rho u v S H\right)_j + \frac{A\Delta x}{\Delta t}(\rho u)$$
(3)

To obtain the transport equation for lateral momentum, a separate control volume is utilized that is placed between the connected volumes, as shown in Fig.6. In deriving the lateral momentum transport equation, it is assumed that the difference in lateral momentum flux is negligible. This is the fundamental assumption of the subchannel method which allows for the arbitrary cross-connection of multiple subchannels. The resulting transport equation is given below.

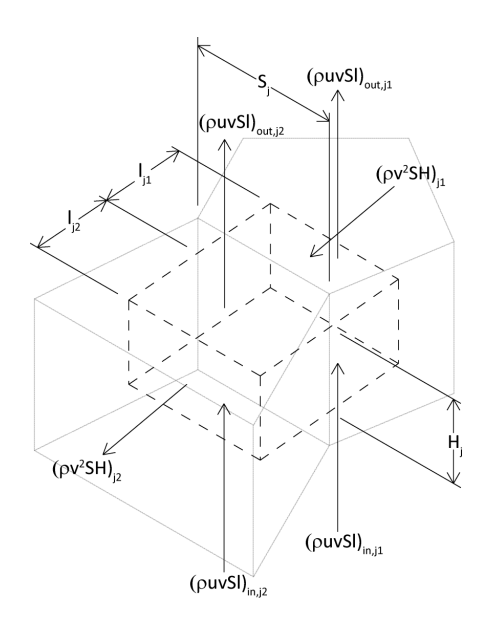


Fig. 6: Control volume used in derivation of lateral momentum equation.

Conservation of Lateral Momentum

$$\frac{SH(l_1 + l_2)}{\Delta t}(\rho v) + (\rho u v S l)_{out,1} + (\rho u v S l)_{out,2} - (\rho u v S l)_{in,1} - (\rho u v S l)_{in,2} 
= (p_1 - p_2)SH - K\rho \frac{|v|v}{2}SH + \frac{SH(l_1 + l_2)}{\Delta t}(\rho v)^0$$
(4)

#### 2.4 Discussion of the transport equations

In solving the transport equations, different quantities are stored at different locations. Thermophysical properties are stored at the cell centers and must be extrapolated to the faces for use in the transport equations. The fluid velocities are stored at the cell faces and utilize the cell centered pressures in the transport equations.

The impact of the crossflow terms appears in Eq. 1 through Eq. 3 as a source on the right hand side. The source is written such that the fluid is assumed to be exiting the volume, but the actual sign of each crossflow source term is dependent on the crossflow junction orientation. A control volume width of zero can be specified, in which case the lateral momentum equation reduces to a force balance between the pressure and friction forces.

Last, it is noted that Eq. 1 through Eq. 3 have been obtained for a control volume with a single inlet junction and a single outlet junction. The actual code is more general and allows for multiple axial connections to a volume. This situation is further complicated when the equations discretized at a single junction have multiple upwind junctions, and the upwind direction can change if a flow reversal occurs. To handle this situation the code specifies the junction as one of eight available classifications, where each junction classification has a unique discretization.

#### 2.5 Constitutive equations

To close the mathematical model, the thermophysical properties of Helium are implemented using the KTA rules which are valid for pressures ranging from 1 bar to 100 bar and from temperatures ranging from 293 K to 1773 K [13].

Darcy friction factors are utilized in the axial momentum equation for Reynolds numbers above 2200. These friction factors are obtained using the formula from Colebrook provided below.

$$\frac{1}{f^{0.5}} = -2.0 \log \left( \frac{e/D}{3.7} + \frac{2.51}{\text{Re } f^{0.5}} \right)$$
 (5)

Several crossflow head loss models are hardcoded into the code for convenience. In addition, the user has the ability of placing a multiplier on the head loss coefficient for use in sensitivity studies. The head loss models available in the code include a constant value, Groehn, and GA. The equations used in the empirical models are given below.

Groehn performed an experimental study of leakage flows between HTGR fuel blocks separated by large wedge shaped gaps, and developed a correlation relating the difference between the mean coolant channel gas velocity above the gap to the velocity below the gap to the pressure difference [14]. This correlation was manipulated by AMEC [15] to yield the equation below for the gap head loss coefficient.

$$K_{gap} = \left(\frac{A_{gap}}{A}\right)^{2} \left[ 3.58 \left(\frac{a}{D}\right)^{-2.3} \cdot 6.33 \left(\frac{A_{gap}}{a \cdot s}\right)^{-1.68} \right]$$
 (6)

Loss coefficient data for crossflow at 2 full scale fuel elements is available from Gulf General Atomics [16]. This data has been fitted by AMEC [8] and manipulated into SI units. The resulting correlation for the gap head loss coefficient is provided below.

$$K_{gap} = 945.18a^{-1.63634} \cdot (a \cdot s)^2 \tag{7}$$

# 3. Solution algorithm

To solve the field equations, the semi-implicit method for pressure linked equations (SIMPLE) algorithm of Patankar [10], is utilized. The SIMPLE algorithm utilizes a pressure correction equation which is obtained by introducing the momentum equations into the conservation of mass equation. In Section 2.4 it was mentioned that different junction arrangements resulted in different discretizations. It will be shown that this does not impact the pressure correction equation. Therefore a single general pressure correction equation can be obtained which is applied to all volumes within the computational domain. The derivation of the pressure correction equation begins with a generalized conservation of mass equation and conservation of momentum equations, where the coefficients in Eq. 9 and Eq. 10 are dependent on the discretization scheme employed.

$$\frac{A\Delta x}{\Delta t}\rho + \sum_{out} (\rho u A)_{out} - \sum_{in} (\rho u A)_{in} + \sum_{j} (\rho v S H)_{j} = \frac{A\Delta x}{\Delta t}\rho^{0}$$
(8)

$$a_{u}u = \sum_{o,j.} a_{o,j.}u_{o,j.} - \sum_{i.j.} a_{i.j.}u_{i.j.} + (p_{i.v.} - p_{o.v.})A + b_{u}$$
(9)

$$a_{v}v = a_{o,g}, v_{o,g} + a_{i,g}, v_{i,g} + (p_{i,v} - p_{o,v})SH + b_{v}$$
(10)

The axial velocity, lateral velocity, and pressure are separated into a guessed value and a correction value. Hence,  $p = p^* + p'$ ,  $u = u^* + u'$ , and  $v = v^* + v'$ . If these values are placed into the momentum equations, then the guessed velocities satisfy the guessed pressure field with the corresponding source and Eq. 9 and Eq. 10 reduce to the following.

$$a_{u}u' = \sum_{o.j.} a_{o.j.}u'_{o.j.} - \sum_{i.j.} a_{i.j.}u'_{i.j.} + (p'_{i.v.} - p'_{o.v.})A$$
(11)

$$a_{v}v' = a_{o.g.}v'_{o.g.} + a_{i.g.}v'_{i.g.} + (p'_{i.v.} - p'_{o.v.})SH$$
(12)

Next is the key simplifying step of the SIMPLE algorithm. The correction terms of the outlet and inlet junctions are dropped and the correction velocities are given by Eq. 13 and Eq. 14.

$$u' = (p'_{i.v.} - p'_{o.v.}) \frac{A}{a_u}$$
 (13)

$$v' = (p'_{i,v} - p'_{o,v}) \frac{SH}{a_v}$$
 (14)

The 14<sup>th</sup> International Topical Meeting on Nuclear Reactor Thermalhydraulics, NURETH-14 Toronto, Ontario, Canada, September 25-30, 2011

Placing Eq. 13 and Eq. 14 into Eq. 8, one arrives at the pressure correction equation.

$$a_{p}p' = \sum_{o.v.} a_{o.v.}p'_{o.v.} + \sum_{i.v.} a_{i.v.}p'_{i.v.} + \sum_{j} a_{j}p'_{o.v.} + b_{p}$$
(15)

with,

$$a_{o,v.} = \rho_{o,j.} \frac{A^{2}_{o,j.}}{a_{u,o.j}}$$

$$a_{i.v.} = \rho_{i.j.} \frac{A^{2}_{i.j.}}{a_{u,i.j}}$$

$$a_{p.} = \sum_{o.v.} a_{o.v.} + \sum_{i.v.} a_{i.v.} + \sum_{j} a_{j.}$$

$$b_{p.} = \frac{(\rho^{0} - \rho)A\Delta x}{\Delta t} + \sum_{i.j} (\rho u^{*} A)_{.j.} - \sum_{o.j} (\rho u^{*} A)_{o.j.} - \sum_{i} (\rho v^{*} S H)_{j}$$

To solve the system of equations initial guessed values are placed into all quantities in order to obtain coefficient matrices, and the momentum equations are solved using the guessed pressure field. The resulting velocity field is used to obtain the source term in the pressure correction equation. After solving the pressure correction equation, the velocity and pressure field is updated and the energy equation is solved. This process is iterated upon until the velocity field satisfies continuity and the correction terms vanish.

# 4. Preliminary validation efforts

As of the current date, a single validation calculation has been performed in which the calculation is compared against experimental data. The calculation is performed for a bypass flow test performed by Kaburaki and Takizuka [17] and represents four full size HTTR fuel elements surrounded by a metal shroud that simulates a 1-mm bypass flow gap with a crossflow gap imposed between the 2<sup>nd</sup> and 3<sup>rd</sup> fuel element. To perform the calculation an initial analytic study was performed to obtain simulation parameters from the data and to investigate pertinent phenomena.

Kaburaki and Takizuka measured the mass flow rate to be 182 g/s. Using the measured mass flow rate and the pressure drop at the interface between the 3<sup>rd</sup> and 4<sup>th</sup> blocks, the form loss coefficient for the combined expansion/contraction is calculated to be approximately 0.3. The pressure drop at the entrance due to fluid acceleration and entrance loss coefficient is obtained by utilizing the value of 9% for the bypass flow, which had been determined by Kaburaki and Takizuka; an entrance form loss coefficient of 0.4 is obtained from the calculation. In a manner similar to the original work of Kaburaki and Takizuka, the hydraulic diameter is adjusted to consider the effect of the insertion of the pressure tube. In combination with a friction factor obtained using the Colebrook equation for a smooth pipe, a hydraulic diameter of 1.6 cm is found to produce a satisfactory slope for the pressure profile.

For the flow between the block and shroud, the pressure drop is obtained using the analytic solution for flow between parallel plates given by Eq. 16, where u is the mean velocity of the fluid, l is the friction length, and t is the gap thickness. The Reynolds number in bypass flow channel has been calculated to be 1730.

$$\Delta p = \frac{12\mu u}{t^2}l\tag{16}$$

Utilizing the analytic solution and the value of 9% for the bypass flow, a bypass flow channel width of 1 mm over-predicts the pressure drop. Adjusting the bypass flow channel width to 1.3 mm produces a pressure drop in the bypass flow channel that is consistent with experimental data. The pressure profiles obtained analytically are displayed in Fig. 7.

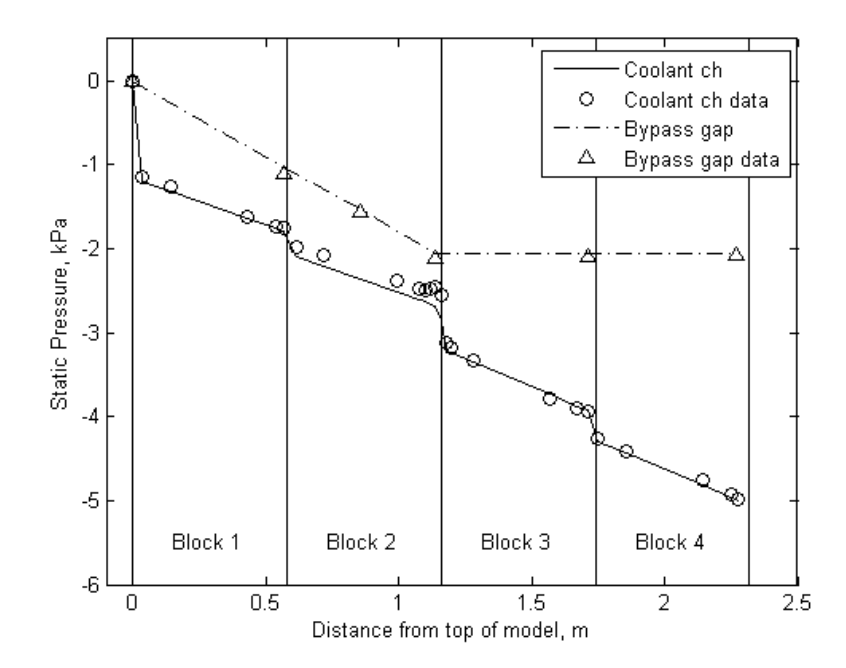


Fig. 7: Comparison of analytic calculation against experimental data of Kaburaki and Takizuka.

The AGREE model is currently a plenum-to-plenum model, where each plenum is modeled as a time-dependent volume meaning that the pressure and temperature within the upper and lower plenum are user-specified as a function of time. The upper plenum is specified to be at atmospheric pressure (101.3 kPa) and at a temperature of 293.15 K. The lower plenum pressure is adjusted to produce a mass flow rate of 182 g/s through the model, which results in a lower plenum pressure of 96.0 kPa.

An expression for the gap crossflow resistance is available in Kaburaki and Takizuka that is a function of the Reynolds number. This function is relatively invariant for bypass flows over 5%. A value of 3.77 corresponds to the measured bypass flow of 9% and is input to the AGREE model.

The results from the analysis with AGREE are shown in Fig. 8. A mass flow rate of 182 g/s with a bypass flow of 11.6% is calculated. The bypass flow over-predicts the 9% value stated by Kaburaki and Takizuka, which was obtained by a flow network calculation, by 2.6%. The data from Kaburaki and Takizuka does not include any information regarding uncertainty in the measurements; therefore, it is difficult to make statements regarding the accuracy of the calculation in regard the physical data. However, it can be observed that the pressure profile in the main coolant and bypass flow channels produced by the AGREE calculation demonstrate the same physical trends as observed in the experimental data. In particular, the large pressure drop attributed to the flow acceleration at the entrance to each flow channel is observed and appears to be correct in magnitude. The major friction losses within the flow channels appear to match the profiles well, where the Colebrook equation is used to obtain the friction factor within the turbulent regime found in the main coolant channel, and laminar flow is observed in the bypass channel. Stagnation in the bypass channel and the resulting flow

acceleration that results from the merging crossflow into the main coolant channel is observed and appears to be correct in magnitude.

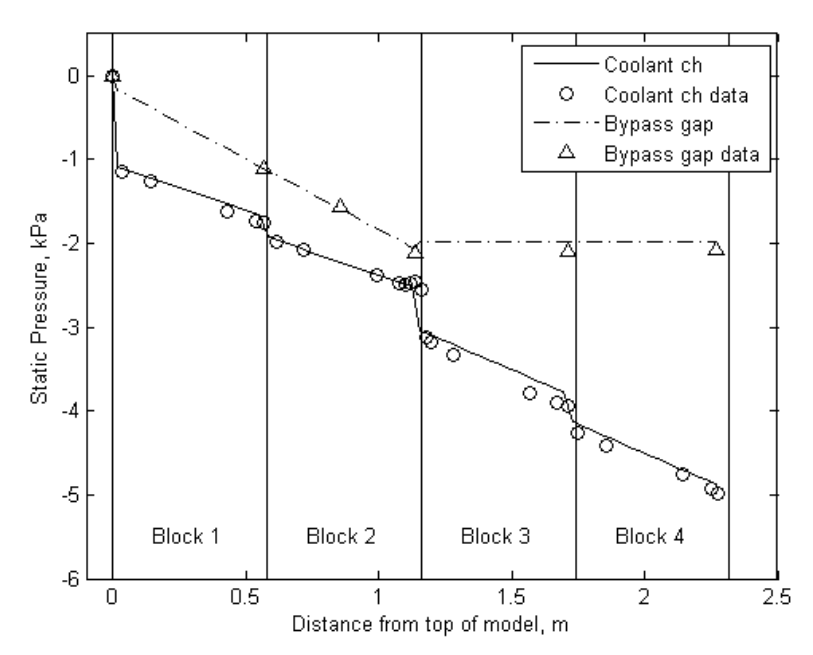


Fig. 8: Comparison of AGREE calculation against experimental data of Kaburaki and Takizuka.

## 5. Conclusions

Currently the PMR core fluids modeling has been implemented into AGREE. Initial validation efforts demonstrate adequate modeling of the physics related to bypass flows in PMRs, but quantitative statements regarding the accuracy of the calculation could not be made with confidence due to the absence of information regarding uncertainty in the data. Efforts are currently underway to implement further modifications into AGREE which are needed to handle the neutronics and heat conduction for the PMR. Further validation calculations are planned where the calculations will be compared against the test data from the High Temperature Test Facility (HTTF) [18]. Additionally, full three-dimensional CFD calculations will be performed in order to investigate the validity of the assumptions imposed on the subchannel model.

## 6. References

- [1] V. Seker, Multiphysics Methods Development for High Temperature Gas Cooled Reactor Analysis, Ph.D Dissertation, Purdue University, December 2007
- [2] T. J. Downar et. al. PARCS: Purdue Advanced Reactor Core Simulator, PHYSOR 2002, Seoul, Korea, October 7-10, 2002
- [3] Next Generation Nuclear Plant Phenomena Identification and Ranking Tables (PIRTs), Volume 1: Main Report NUREG/CR-6944, Vol.1. March 2008.

- [4] Prioritization of VHTR System Modeling Needs Based on Phenomena Identification, Ranking, and Sensitivity Studies, ANL-GenIV-071. April 2006.
- [5] B.L. Strain, FLOPSY II A Digital Computer Program for Calculating Flow and Pressure Drops in Hydraulic Networks. KAPL-3030, 1965.
- [6] R.B. Vilim, GAS-NET: A Two-Dimensional Network Code for Prediction of Core Flow and Temperature Distribution in the Prismatic Gas Reactor. ICAPP 2007, Nice, France, May13-18, 2007.
- [7] R. Stainsby, A. Grief, and W. Worsley, Investigation of Local Heat Transfer Phenomena in a Prismatic Modular Reactor Core. NR001/RP/001 R1, AMEC NSS Limited. March 30, 2009.
- [8] J.P Simoneau, J. Champigny, B. Mays, and L Lommers, Three-dimensional simulation of the coupled convective, conductive, and radiative heat transfer during decay heat removal in an HTR. Nuc. Eng. and Des. vol. 237, 2007, pp. 1923-1937.
- [9] W.D. Pointer, C.H. Lee, J.W. Thomas, Y.S. Jung, and W.S. Yang. Steady-State, Whole-Core VHTR Simulation with Consistent Coupling of Neutronics and Thermo-fluid Analysis. ANL-GenIV-121. Sept. 2009.
- [10] S.V. Patankar, Numerical Heat Transfer and Fluid Flow. p. 88-90 and p. 126-131, Hemisphere Publishing Co.1980.
- [11] C.W. Stewart et. al., COBRA-IV: The Model and the Method. BNWL-2214, Battelle Pacific Northwest Laboratories. July 1977.
- [12] C.W. Stewart et. al., VIPRE-01: A Thermal-Hydraulic Analysis Code for Reactor Cores, EPRI NP-2511-CCM, Volume 1, Rev. 2, July 1985.
- [13] Reactor Core Design for High-Temperature Gas-Cooled Reactor, Part 1: Calculation of the Material Properties of Helium. KTA 3102.1. Nuclear Safety Standards Commission (KTA). June 1978.
- [14] H.G. Groehn, Estimate of Cross Flow in High Temperature Gas-Cooled Reactor Fuel Blocks, Nuclear Technology, vol. 56. Feb. 1982, pp. 392-400.
- [15] Investigation of Local Heat Transfer Phenomena in a Prismatic Modular Reactor Core. NR001/RP/001 R1, AMEC NSS Limited. March 30, 2009.
- [16] Analysis of the Multicolumn Flow Distribution Test Data. GAMD-8423. Gulf General Atomics Inc. June 1968.
- [17] H.Kaburaki and T. Takizuka. Effect of Crossflow on Flow Distributino on HTGR Core Column. Journal of Nuclear Science and Technology, vol. 24, July 1987, pp. 516-525.
- [18] R.B. Jackson, B. Woods, and K. Keady, Scaling Analysis for Depressurization of High-Temperature Test Facility. ANS Transactions, vol. 102. pp. 609-610.